

Mausumi Ghosh, Niels Denkert, Maren Reuter, Jessica Klümper, Katharina Reglinski, Rebecca Peschel, Wolfgang Schliebs, Ralf Erdmann\* and Michael Meinecke\*

# Dynamics of the translocation pore of the human peroxisomal protein import machinery

<https://doi.org/10.1515/hsz-2022-0170>

Received April 30, 2022; accepted July 5, 2022;  
published online August 18, 2022

**Abstract:** Peroxisomal matrix proteins are synthesized on cytosolic ribosomes and imported in a posttranslational manner. Intricate protein import machineries have evolved that catalyze the different stages of translocation. In humans, PEX5L was found to be an essential component of the peroxisomal translocon. PEX5L is the main receptor for substrate proteins carrying a peroxisomal targeting signal (PTS). Substrates are bound by soluble PEX5L in the cytosol after which the cargo-receptor complex is recruited to peroxisomal membranes. Here, PEX5L interacts with the docking protein PEX14 and becomes part of an integral membrane protein complex that facilitates substrate translocation into the peroxisomal lumen in a still unknown process. In this study, we show that PEX5L containing complexes purified from human peroxisomal membranes constitute water-filled pores when reconstituted into planar-lipid membranes. Channel characteristics were highly dynamic in terms of conductance states, selectivity and voltage- and substrate-sensitivity. Our results show that a PEX5L associated pore exists in human peroxisomes, which can be activated by receptor-cargo complexes.

---

Mausumi Ghosh, Niels Denkert, and Maren Reuter contributed equally to this work.

---

**\*Corresponding authors:** Ralf Erdmann, Institute of Biochemistry and Pathobiochemistry, Ruhr University Bochum, D-44780 Bochum, Germany, E-mail: Ralf.Erdmann@rub.de. <https://orcid.org/0000-0001-8380-0342>; and Michael Meinecke, Biochemistry Center (BZH), Heidelberg University, D-69120 Heidelberg, Germany; and Institute for Cellular Biochemistry, University Medical Center Göttingen, D-37073 Göttingen, Germany, E-mail: michael.meinecke@bzh.uni-heidelberg.de. <https://orcid.org/0000-0003-1414-6951>

**Mausumi Ghosh and Niels Denkert**, Biochemistry Center (BZH), Heidelberg University, D-69120 Heidelberg, Germany; and Institute for Cellular Biochemistry, University Medical Center Göttingen, D-37073 Göttingen, Germany. <https://orcid.org/0000-0002-2551-0360> (N. Denkert)

**Maren Reuter, Jessica Klümper, Katharina Reglinski, Rebecca Peschel and Wolfgang Schliebs**, Institute of Biochemistry and Pathobiochemistry, Ruhr University Bochum, D-44780 Bochum, Germany. <https://orcid.org/0000-0003-0041-5268> (R. Peschel)

**Keywords:** channel; peroxisome; protein translocation pore.

## Introduction

Peroxisomes are versatile, spherical organelles, which are surrounded by a single lipid bilayer and can be found in all eukaryotic cells (van den Bosch et al. 1992). They comprise a dynamic enzyme content that varies depending on current cellular needs (Wanders et al. 2018). Conserved functions include the detoxification of hydrogen peroxide by catalase and degradation of fatty acids by  $\beta$ -oxidation enzymes. In human cells, peroxisomes are involved in lipid synthesis, such as bile acids, plasmalogens or cholesterol (Rucktäschel et al. 2011; Wanders et al. 2018). The physiological importance of peroxisomes in human cells is emphasized by the severity of diseases occurring upon peroxisomal defects in biogenesis (Cheillan 2020; Wanders 2018; Waterham et al. 2016). Peroxisomes do not contain any kind of transcription or translation machinery. Hence, all peroxisomal proteins are synthesized in the cytosol and need to be imported into the organelle post-translationally (Goldman et al. 1978; Lazarow et al. 1985). Therefore, peroxisomal matrix proteins are equipped with a peroxisomal targeting signal (PTS), of which two types, the carboxyterminal PTS1 and the amino-terminal PTS2 are most common (Gould et al. 1989; Kunze 2020; Neuberger et al. 2003; Swinkels et al. 1991). Mechanisms of peroxisomal biogenesis are well conserved among organisms as indicated by ubiquitous usage of targeting signals and the functional and structural conservation of peroxins, or PEX-proteins, which are facilitating and maintaining the biogenesis and homeostasis of these organelles. The central part of the import machinery for matrix proteins is the soluble import receptor PEX5, which recognizes PTS1 cargo proteins in the cytosol and transports them to the peroxisome (Brocard et al. 1994; Dodt et al. 1995). Proteins containing a PTS2 are recognised by the import receptor PEX7, which requires additional co-receptors for peroxisomal targeting (Kunze et al. 2015; Schliebs et al. 2006). In humans, this co-receptor is a longer splice variant of PEX5, named PEX5L (as outlined above) (Otera et al. 2000), therefore both import pathways converge at the

level of PEX5L. Once the receptor-cargo complex reaches the peroxisomal membrane, PEX5 interacts with a docking-complex, consisting of the membrane peroxins PEX13 and PEX14, and in yeast also Pex17. Remarkably, upon binding to the docking complex, PEX5 integrates into the membrane and becomes a central constituent of the import complex (Kerssen et al. 2006). In yeast this was shown to lead to the formation of a transient import pore (Meinecke et al. 2010). However, the mechanism of membrane translocation of folded and even oligomerized matrix proteins and cargo release remains to be unravelled. After cargo dissociation, unloaded PEX5 is extracted from the membrane and released back into the cytosol. Thus, PEX5 is a cycling receptor, shuttling between a cytosolic and an integral membrane form (Erdmann et al. 2005). In yeast, the recycling requires the Pex8p-dependent association of the importomer consisting of the docking complex and the import pore with the so-called RING finger complex, which is conserved among species and consists of the ubiquitin ligases PEX2, PEX10 and PEX12 (Agne et al. 2003; Platta et al. 2007). With the help of E2-enzymes E2D1/2/3 in mammals, Pex4 and its membrane anchor Pex22 in yeast, Ubiquitin is transferred onto PEX5. Then the ubiquitin moiety is recognized by the PEX1/PEX6/PEX26 (or Pex15 in yeast) AAA-complex, which extracts the receptor from the membrane in an ATP-dependent manner (Grou et al. 2008; Platta et al. 2005).

With the exception of Pex8, Pex17, Pex22 and auxiliary receptors Pex18 and Pex21 of the PTS2 pathway, all components of the yeast peroxisomal import machinery have been shown to be present also in humans. Here we show that human peroxisomes harbor PEX5L-associated gated translocation pore. PEX5L containing complexes purified from human peroxisomal membranes constitute highly dynamic water-filled pores when reconstituted into planar lipid membranes.

## Results

In yeast, we found that matrix import of peroxisomal proteins most likely occurs through large, substrate sensitive pores (Meinecke et al. 2010, 2016). For PTS1 containing substrates, Pex5p, possibly together with Pex14p, was identified to be a major part of this pore (Meinecke et al. 2010), while for PTS2 substrates Pex18p, Pex14p and Pex17p are major constituents of the protein conducting channel (Montilla-Martinez et al. 2015).

To identify a putative pore forming activity within the human import machinery, we established an approach to affinity-purify PEX5 as the supposedly central component

of the pore. To this end, we constructed a cell line that expressed Protein A-tagged PEX5L, which contained a TEV cleavage site between the tag and the protein. Membranes were solubilized by mild digitonin treatment to preserve association of integral membrane protein complexes. Affinity purification of PEX5-complexes via IgG Sepharose was performed and complexes were eluted by TEV protease cleavage (Figure 1A).

SDS-PAGE analysis of the PEX5 eluates of membrane proteins and soluble proteins revealed distinct polypeptide composition of cytosolic and peroxisomal Protein A-tagged PEX5 (Figure 1B and C and Supplementary Figure 1). The predominant PEX5-associated 60 kDa polypeptide at the membrane most probably represents PEX14. Several polypeptides with estimated masses of around 80, 50, 40 and 30 kDa cofractionate with the cytosolic PEX5. Although the identity of cytosolic binding partners has not been addressed in this study, it can be speculated that the cytosolic binding partners most likely represent abundant cargo proteins with high affinity towards the PTS1 receptor. This is further corroborated by immunoblotting, demonstrating association of catalase with the PTS1 receptor (Figure 1C). No cargo proteins but membrane-bound peroxins including PEX13, PEX12 and PEX1 were detected in the PEX5 membrane eluate. Interestingly, PEX6, which forms a functional complex with PEX1, could not be identified, suggesting that the interaction between the two human AAA peroxins is not as stable as suggested by structural analyses (Blok et al. 2015; Ciniawsky et al. 2015; Gardner et al. 2015; Saffert et al. 2017).

The TEV eluate of solubilized membrane complexes, was used for a mixed detergent mediated reconstitution protocol to incorporate integral membrane protein complexes into liposomes. Incorporation success was monitored by flotation and carbonate extraction resistance assays using PEX5 and PEX14 as marker proteins (Supplementary Figure 2).

Proteo-liposomes containing the PEX5-complex were subsequently analyzed for pore-forming activity using the planar lipid bilayer technique (Denkert et al. 2017; Vasic et al. 2020). Ion-channel activity could readily be detected though, the electrophysiological characteristics were rather dynamic (Figure 2). Channels showed voltage dependent gating with a large variety of different conductance states from 40 up to 550 pS (Figure 2A and B). A mild ion-selectivity was measured that even changed according to the open state of the channel (Figure 2C). Interestingly, conductance states, dynamic gating and mild but changing selectivity was also observed in the past for the PTS1 specific import channel in yeast of which Pex5 is a major constituent (Meinecke et al. 2010). To rule

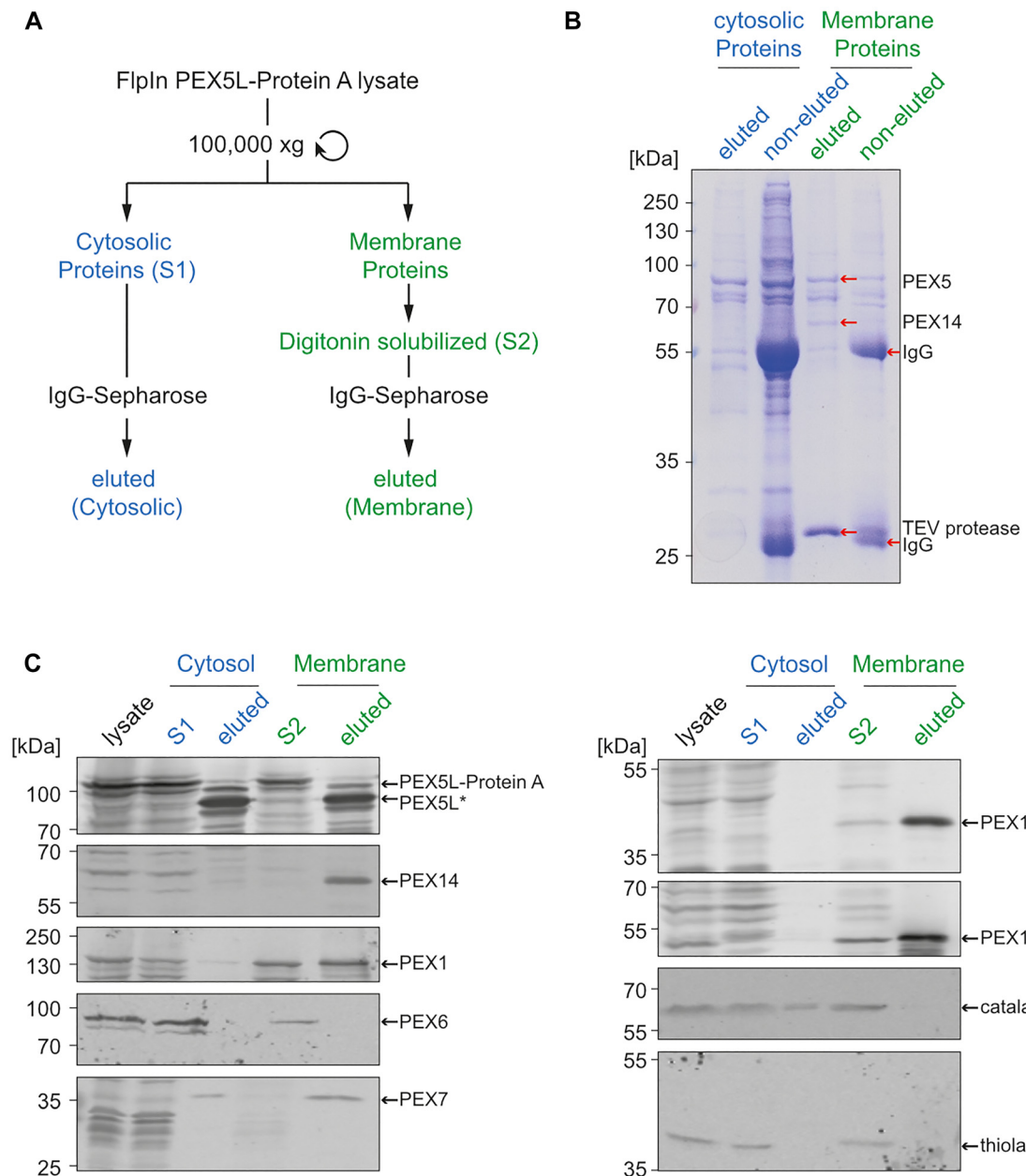


**Figure 1:** Purification of PEX5-containing membrane complexes.

(A) Scheme of affinity-purification of cytosolic and membrane-bound subcomplexes of human Protein A-fused PEX5L. (B) Colloidal Coomassie stained SDS-PAGE of the TEV-protease eluates of cytosolic and membrane-bound PEX5L. To monitor the efficacy of the digitonin-solubilization and TEV-proteolytic cleavage, the IgG-sepharose column material was subsequently incubated with SDS containing buffer to analyze remaining proteins. (C) Immunoblot analysis of the purification profile. The lysates, loads (S1 and S2) and corresponding eluates were investigated for the presence of components of the peroxisomal import machinery and matrix proteins with indicated antibodies.

out that the observed heterogeneity is due to multiple inserted channels displaying different characteristics, we reduced the proteoliposome concentration prior to fusion with the bilayer. Consequently, channel fusions were far less frequent but the fusions that occurred were predominantly single channels. Upon closer analysis of the single-channel characteristics we were able to

differentiate between two different states. We measured channels with rather small conductivity of about 75 pS with very rare events up to about 400 pS (Figure 2D–G). A second population also displayed the prominent small conductance state but additionally showed more frequent larger gating events corresponding to conductance states between 400 and 900 pS (Figure 2H–J). Again, both channel

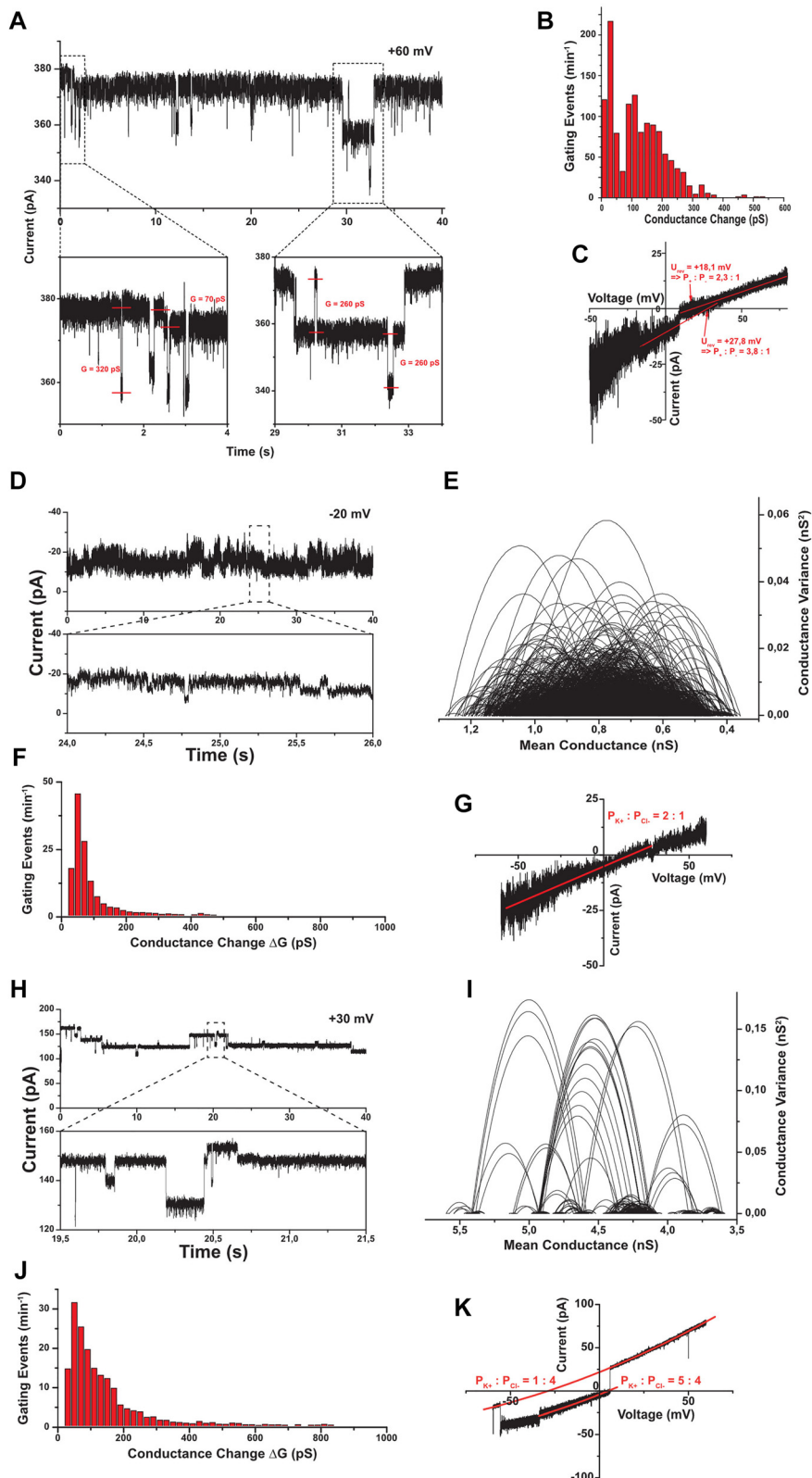


**Figure 2:** Pore forming activity of PEX5 complexes.

(A) Current traces of PEX5 complex containing bilayers under symmetric buffer conditions at indicated holding potential. Zoom plots show distinct voltage dependent gating with indicated conductance states. (B) Conductance state histogram of voltage dependent gating of PEX5 complexes from current recordings at different holding potentials and from at least three independent fusion events. (C) Current–voltage

populations displayed a mild and changing ion selectivity (Figure 2G and K).

Since the size exclusion chromatogram of detergent solubilized PEX samples indicated the appearance of different complex assemblies (data not shown), we asked whether the two observed channel populations might correspond to PEX complexes in different stages of the import cycle. To simulate a state in which the putative import pore is in contact with cargo molecules, we incubated PEX complex containing proteoliposomes with PEX5-PEX7-Cargo complexes that were purified from soluble fractions of cell lysates devoid of membranes as shown in Figure 1. After incubation with the soluble PEX5-complex, the proteoliposomes were again subjected to electrophysiological characterization. The resulting channel characteristics were comparable to the ones we observed before for the PEX complexes in a high conductance state. Voltage-dependent gating showed the prominent small conductance state of about 75 pS and additionally much larger gating events corresponding to conductance states between 400 and 1000 pS were observed (Figure 3A and B). Ion-selectivity was mild and changed upon gating (Figure 3C). Comparing conductance state distribution histograms of PEX complexes in the absence and presence of soluble cargo containing substrates indicates that the addition of substrates leads to a transition of the complex activity towards a high conductance state configuration (Figure 3D). Consequently, after substrate incubation no channel activities that only displayed low conductance states could be observed (Figure 3E). In conclusion, the results suggest that the human PEX5 complexes have pore-forming capabilities. If the different channel populations represent complexes of different composition or different activity states of the same complex remains to be analyzed. Since the addition of cargo complexes to membrane-integrated PEX complexes led to a shift of activities where only the high conductance state complex was detectable, it is tempting to speculate that this state represents a transport

active conformation of the complexes. As a specificity test and to rule out unspecific contamination during the purification processes, we performed fusion experiments with all used samples. Whereas channel fusions could be observed with membrane integrated PEX5 complexes in the absence and presence of soluble cargo complexes, no fusion were observed when using a mock Protein A affinity purification from cell lines of untagged wild type PEX5 in the absence and presence of soluble cargo or when only using soluble cargo complexes (Figure 3F).

## Discussion

In this study, affinity-purified subcomplexes of membrane-solubilized ProteinA-tagged PEX5 were reconstituted into proteo-liposomes and fused with planar lipid-bilayers. Electrophysiological measurements revealed the existence of at least two distinct open channel populations of predominantly low and high conductance. The low conductance channels open to an estimated diameter (for details of the calculation see materials and methods) of maximal 2 nm (~420 pS), whereas the high-conductance pores exhibit diameters of around 3 nm (>800 pS). Remarkably, upon preincubation with affinity-purified PEX5 complexes from the cytosol, the low-conductance channels shift into high-conductance states with estimated maximal pore-diameters of 3.3 nm (~950 pS). The increase in pore size upon preincubation with cytosolic PEX5-complexes might be explained by an incorporation of the receptor-cargo complexes into pre-existing import channels at the membrane. It should be noted however, that even the low conductance channel population in the absence of additional PEX5-cargo, shows an intrinsic ability to gate in higher conductance state, though only in rare events.

The existence of two convertible states of human import channels is in line with results obtained for membrane-associated yeast Pex5 before and after incubation with

---

relationship of a PEX5 complex under asymmetric buffer conditions. Linear fits show the reversal potential which is the basis for the indicated cation to anion selectivity, calculated via the Goldman–Hodgkin–Katz equation. (D–G) Electrophysiological characteristics of channels displaying mainly low conductance state gating. (D) Current trace of a channel displaying mainly low conductance state gating under symmetrical buffer conditions at indicated holding potential. (E) Mean conductance differences plotted against their variance of the corresponding current trace D. (F) Conductance state histogram of voltage dependent gating of PEX5 complexes from current recordings at different holding potentials and from at least three independent fusion events. (G) Current–voltage relationship of PEX5 complexes recorded under asymmetric buffer conditions with indicated cation to anion selectivity. (H–K) Electrophysiological characteristics of channels displaying high conductance state gating. (H) Current trace of a channel displaying mainly low conductance state gating under symmetrical buffer conditions at indicated holding potential. (I) Mean conductance differences plotted against their variance of the corresponding current trace H. (J) Conductance state histogram of voltage dependent gating of PEX5 complexes from current recordings at different holding potentials and from at least three independent fusion events. (K) Current–voltage relationship of PEX5 complexes recorded under asymmetric buffer conditions with indicated cation to anion selectivity.

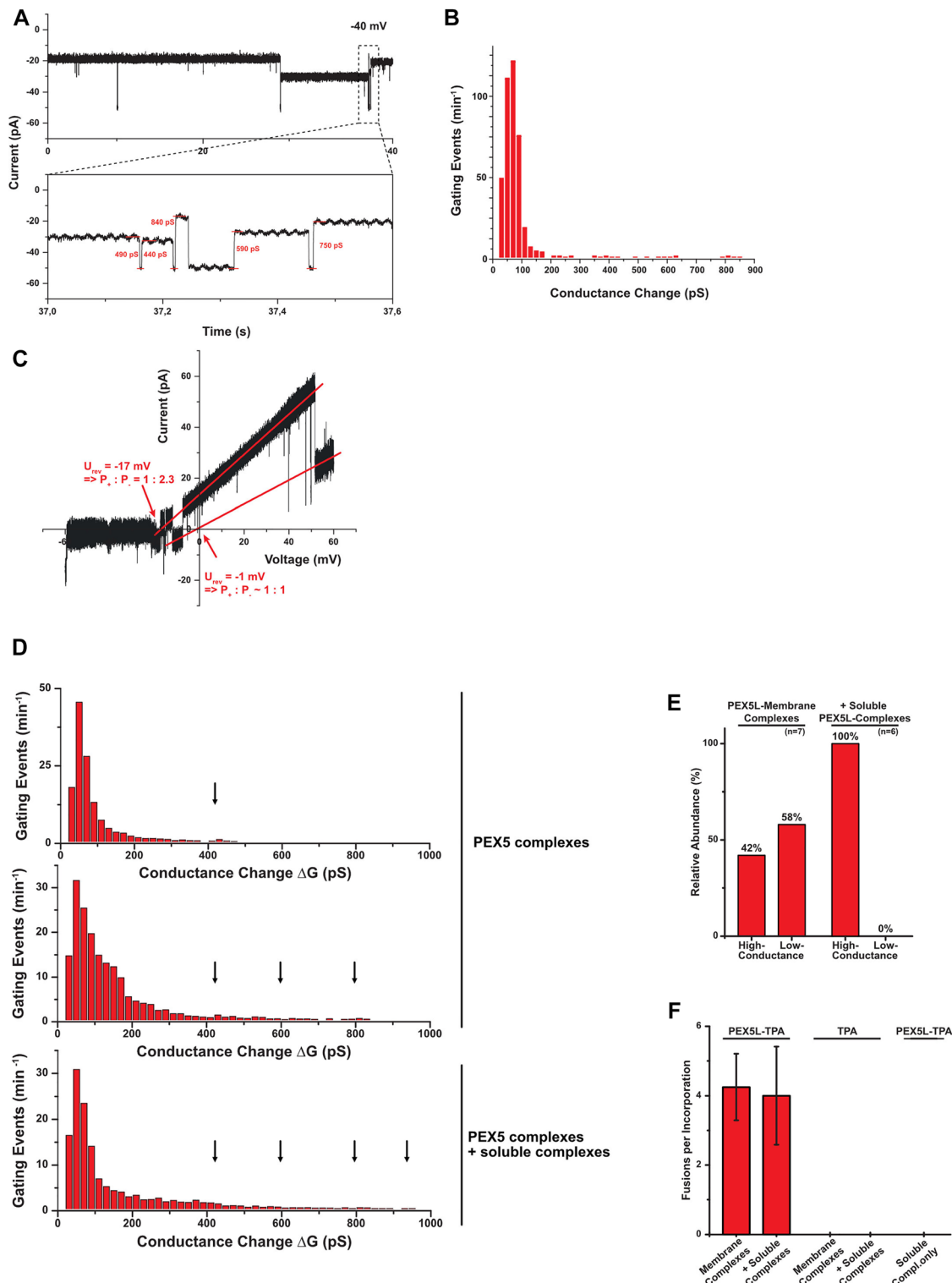


**Figure 3:** PEX5 complex activity is cargo sensitive.

(A) Current traces of PEX5 complex incubated with soluble PEX5-cargo complexes fused to bilayers and measured under symmetric buffer conditions at indicated holding potential. Zoom plots show distinct voltage dependent gating with indicated conductance states. (B) Conductance state histogram of voltage dependent gating of cargo activated PEX5 complexes from current recordings at different holding potentials and from at least three independent fusion events. (C) Current–voltage relationship of a cargo activated PEX5 complex under asymmetric buffer conditions with indicated reversal potentials and calculated cation to anion selectivity. (D) Conductance state histograms of PEX5 complexes in the absence (upper two panels) and presence (lower panel) of PEX5-cargo complexes. Arrows indicate increasing conductance states. Conductance states were gathered from current recordings at different holding potentials and from at least three different channel insertions. (E) Statistical representation of the relative abundance of channels displaying either mainly small conductance states or also frequent larger conductance states, respectively. (F) Fusion rates of indicated samples show that only PEX5 complexes purified from membranes lead to channel activities.

cytosolic receptor cargo complexes (Meinecke et al. 2010). Remarkably, the main conductance of the yeast membrane-bound Pex5-complex without cargo had a pore-diameter of around 0.6 nm, while incubation with receptor-cargo complexes induced conductance states corresponding to about 9 nm channel size diameter (Meinecke et al. 2010). The estimated ground-state of the yeast PEX5 channel of 0.6 nm assures the membrane integrity of the yeast peroxisomal membrane. The human PEX5 channel is also mainly found to gate in this small (about 0.6 nm), low conductance state, while it sometimes shows larger gating events (about 2 nm). If the human PEX5 channel with diameter of 2 nm would permanently exist in human peroxisomes, peptides and metabolites could be released into cytoplasm. On the other hand, the estimated pore-diameter of 3.3 nm for the human translocon is not wide enough to explain the import of large folded and oligomeric matrix proteins into human peroxisomes (Montilla-Martinez et al. 2015; Walton et al. 1995). Our data are clear in that the human peroxisomes contain a large PEX5-associated protein translocation pore, but our experimental system might not trigger the full opening of the channel. One possibility would be that the pore assembles on demand according to the size of substrate and that wider pore-openings might be observed when very large or oligomerized substrates are bound to the import receptor. It is however possible that the low range between minimal and maximal opening of the human PEX5 channel rather results from the different properties of human PEX5 in comparison to its yeast counterpart. In contrast to yeast Pex5, which contains one binding site for the N-terminal domain of Pex14, the human PEX5 contains at least 8 binding sites for PEX14 (Neuhaus et al. 2014; Otera et al. 2002; Saidowsky et al. 2001). Thus, the size and stoichiometry of human PEX5-PEX14 complexes could be more heterogeneous. Interestingly, the Coomassie stain of the membranous PEX5 fraction (Figure 1B) indicates a 1:1 stoichiometry of PEX5 and PEX14, which is in line with the molar ratio of the two proteins in the yeast translocation pore. This is in accordance with a model previously proposed, which favours successive binding of PEX5 single sites to PEX14 rather than simultaneous binding of all eight PEX5 sites to several PEX14 (Emmanouilidis et al. 2016; Neuhaus et al. 2014). It might well be that in our system, gating of the pore is regulated by additional factors and the maximum pore size has not yet been reached. It also should be noted that yeast complexes were analysed from pure size-exclusion chromatography purified fractions constituting mainly Pex5 and Pex14 in a 1 to 1 molar ratio (Meinecke et al. 2010). The heterogeneity of the affinity-purified human PEX5 is further indicated by immunoblot analysis (Figure 1), showing that the human preparation contains various PEX5 interacting proteins, in

particular the membrane-bound peroxins PEX1, PEX13 and the RING-finger peroxin PEX12, which might also have an influence on the pore size.

As the human PEX5L is also associated with the PTS2 receptor PEX7, we can't rule out that the characterized human pores resemble the yeast PTS2 pore. The yeast PTS2 pore is less flexible and seems only to exist in a constitutively open state of around 4 nm diameter (Montilla-Martinez et al. 2015), which would resemble some properties of the human pore.

Further separation and purification of PEX5 sub-complexes, more insight into the role of the eight WxxxxF-motifs and maybe other factors in gating seem to be required to explain the differences of the yeasts and human import pores.

This study shows that a highly dynamic, possibly transient pore is a well conserved feature of yeast and human PEX5 mediated import into peroxisomes. Our data suggest that high conductance states and thus opening of the human pore is induced by incubation with receptor-cargo complexes. This might be accomplished by incorporation of soluble PEX5-cargo complexes into pre-existing membrane-embedded PEX5 complexes. Our data show that the principle mechanisms of the import of matrix proteins, in particular the existence of a large, water-filled protein conducting channel for peroxisomal matrix proteins, possibly with PEX5 and PEX14 as central constituents, is conserved among species, from yeast to humans.

## Materials and methods

### Cultivation of human FlpIn cells

A FlpIn cell line stably expressing PEX5L-Protein A was generated as described before (Bharti et al. 2011). Cells were cultivated in Dulbecco's modified eagle medium (DMEM) with high glucose, supplemented with 10% (v/v) FCS (both purchased from Sigma Aldrich), 2 mM L-glutamine and 1% (v/v) Penicillin (10 U/ml)/Streptomycin (10 µg/ml) (purchased from Gibco), at 37 °C in a humidified atmosphere containing 8.5% CO<sub>2</sub>. For maintenance, cells were grown in T75 flasks, while for complex isolations they were large scale cultivated in *Triple Desk* T500 flasks (Thermo Scientific). Once cells reached a confluence of 90%, they were trypsinized and harvested by centrifugation at 200×g for 7 min. For each complex isolation, cells from 18 *Triple Desk* flasks were used. Sedimented cells were frozen in liquid nitrogen and stored at -80 °C until use.

### Isolation of PEX5 complexes

The FlpIn PEX5L-Protein A cell line was cultivated in *Triple Desk* flasks and harvested as described before. The pellet was resuspended in lysis buffer (0.2 M HEPES, 1 M potassium acetate, 50 mM magnesium

acetate, pH 7.5; 20 ml per 10 g pellet) supplemented with protease inhibitors (8 mM Antipain, 0.3 mM Aprotinin, 1 mM Bestatin, 5 mM Leupeptin, 15 mM Pepstatin, 10 mM Chymostatin, 1 mM Phenylmethylsulfonyl fluoride, 5 mM sodium fluoride, 1 mM Benzamidine hydrochloride). Lysis was performed using glass beads (0.5 mm diameter, 3 g beads per 1 g cell pellet), which afterwards were separated from the lysate by centrifugation for 5 min at 1500g (rotor SX4750A, Beckman Coulter) and 4 °C. The obtained lysate was submitted to ultracentrifugation at 100,000g and 4 °C for 1 h (rotor SW 41 Ti, Beckman Coulter). The resulting supernatant was used for isolation of cytosolic complexes, while the pellet was solubilized for 1 h at 4 °C in lysis buffer as before, containing additional 5% glycerol and 1% digitonin. Following a second 100,000g centrifugation at 4 °C for 1 h, the second supernatant was used for the isolation of membrane protein complexes. The protein content of both supernatants was determined, and each supernatant was incubated with IgG-Sepharose beads (13 µl per 10 mg protein) for 18 h at 4 °C. The IgG-Sepharose was sedimented by centrifugation for 5 min at 1500 g (rotor SX4750A, Beckman Coulter) and 4 °C and washed with wash buffer (0.2 M HEPES, 1 M potassium acetate, 50 mM magnesium acetate, pH 7.5, supplemented with 8 mM Aprotinin, 1 mM Bestatin, 5 mM Leupeptin, 15 mM Pepstatin and 1 mM Phenylmethylsulfonyl fluoride), either containing 0.2% digitonin (for membrane complexes) or no detergent (for cytosolic complexes). The sedimented Sepharose was resuspended in < 1 ml of the corresponding wash buffer and transferred to a centrifugation column (“Mobicol F” with 35 µm filter, Mobitec). The beads were washed 10 times with the corresponding washing buffer by centrifugation at 100g and 4 °C for 30 s. For elution via the TEV protease, 110 U protease (AcTEV™ protease, Invitrogen) were added for every 100 µl IgG-Sepharose and incubated for 2 h at 16 °C and 350 rpm. The Sepharose was sedimented by centrifugation for 1 min at 100g, 4 °C and the corresponding supernatant saved as eluate. The Sepharose was washed twice with two column volumes of the respective wash buffer, and washing fractions were combined with the eluate.

### Preparation of PEX5L proteoliposomes

All lipids used for preparation of liposomes were purchased from Avanti Polar Lipids. The lipid mixture for preparation of liposomes contained 70% L-a-phosphatidylcholine and 30% L-a-phosphatidylethanolamine. Lipid stocks were prepared in methanol/chloroform mixture and dried under constant nitrogen flow to a final concentration of 12 mM. To generate unilamellar vesicles, dried lipid films were resolubilized in 150 mM KCl, 10 mM HEPES pH 7.4 buffer and subjected to seven freeze-and-thaw cycles. The obtained lipid vesicles were extruded through a PVDF filter with pore diameter of 200 nm and used for protein reconstitution. To incorporate PEX5L, liposomes were partially solubilized with 0.2% Digitonin, 0.5% DDM and 3× digitonin buffer and incubated for 5 min on ice. Purified SEC fraction of hPEX5L were added to solubilized liposomes and then incubated for 30 min on ice to allow spontaneous protein insertion. The incorporation process was promoted by removing the detergent from the mixture using 80 µl of Calbiosorb (Calbiochem) per 50 µl lipids, washed with methanol followed by 150 mM KCl, 10 mM HEPES pH 7.4. Calbiosorb were added to the sample mix, incubated on wheel for 2 h at 4 °C and proteoliposomes were separated from the Calbiosorb.

### Liposome flotation assay and sodium carbonate extraction

Flotation assay was performed as described in detail before (Taranenko et al. 2017). For Flotations were performed in non-ionic Histodenz density gradients (Sigma-Aldrich). Proteoliposomes were placed on the bottom of the ultracentrifugation tubes, and the non-continuous 40/20/10/5/2% Histodenz density gradient was built up from high density toward low. Proteoliposome containing gradients were subjected to centrifugation for 1 h at 150,000g and 4 °C. Subsequently, gradients were dissected into separate fractions, precipitated with 10% TCA, and analysed by SDS-PAGE and immunoblotting. For sodium carbonate extraction, liposomes containing interfaces of the Histodenz layers were collected, incubated with ice-cold 20 mM Na<sub>2</sub>CO<sub>3</sub> for 30 min on ice, and centrifuged for 30 min at 150,000g and 4 °C. Total amounts of pellets and TCA-precipitated supernatants were analysed by SDS-PAGE.

### Electrophysiological characterization of PEX5L

Electrophysiological characterization of PEX5L was carried out using the planar lipid bilayer technique, as described in detail before (Domanska et al. 2010; Guan et al. 2019). Electrical current recordings were performed using Ag/AgCl electrodes in glass capillary tubes, embedded in a 2 M KCl agar-bridge. The electrode in the trans-chamber was connected to the headstage (CV-5-1GU) of a Geneclamp 500B current amplifier (Molecular Devices, CA, USA) acting as a reference electrode and electrode in the cis-chamber acting as ground. Data were acquired using a Digidata 1440A A/D converter and recorded using the AxoScope 10.3 and Clampex 10.3 software (Molecular Devices). Data analysis was carried out using OriginPro 8.5G (OriginLab, MA, USA) and R packages stepR (Hotz et al. 2013 IEEE Transactions on Nano-Bioscience) and dbacf. PEX5L-proteoliposomes were inserted into the planar lipid bilayer by osmotic driven fusion in asymmetric buffer condition with 250 mM KCl, 10 mM MOPS, pH 7.0 in the cis-chamber and 20 mM KCl, 10 mM MOPS, pH 7.0 in trans-chamber. After incorporation of hPEX5L into the planar lipid bilayer, both of the chambers were perfused with 250 mM KCl, 10 mM MOPS, pH 7.0 to attain symmetrical buffer conditions and voltage-clamp recordings as well as voltage-ramps were performed. Voltage ramps were recorded from -60 to +60 mV and the current-voltage relationship was plotted. Current traces were recorded at constant voltage for 1 min. Channel diameter: the diameter of the pore was calculated from measured stable conductance states. Therefore, we took a cylindrical pore with a restriction zone of 1 nm in length as the basis, and assumed a fivefold higher solution resistance within the pore than in the bulk medium as described before (Smart et al. 1997).

**Author contributions:** All the authors have accepted responsibility for the entire content of this submitted manuscript and approved submission.

**Research funding:** None declared.

**Conflict of interest statement:** The authors declare no conflicts of interest regarding this article.

## References

Agne, B., Meindl, N.M., Niederhoff, K., Einwachter, H., Rehling, P., Sickmann, A., Meyer, H.E., Girzalsky, W., and Kunau, W.H. (2003). Pex8p: an intraperoxisomal organizer of the peroxisomal import machinery. *Mol. Cell.* 11: 635–646.

Bharti, P., Schliebs, W., Schievelbusch, T., Neuhaus, A., David, C., Kock, K., Herrmann, C., Meyer, H.E., Wiese, S., Warscheid, B., et al. (2011). PEX14 is required for microtubule-based peroxisome motility in human cells. *J. Cell Sci.* 124: 1759–1768.

Blok, N.B., Tan, D., Wang, R.Y., Penczek, P.A., Baker, D., DiMaio, F., Rapoport, T.A., and Walz, T. (2015). Unique double-ring structure of the peroxisomal Pex1/Pex6 ATPase complex revealed by cryo-electron microscopy. *Proc. Natl. Acad. Sci. U.S.A.* 112: E4017–E4025.

Brocard, C., Kragler, F., Simon, M.M., Schuster, T., and Hartig, A. (1994). The tetratricopeptide repeat-domain of the PAS10 protein of *Saccharomyces cerevisiae* is essential for binding the peroxisomal targeting signal-SKL. *Biochem. Biophys. Res. Commun.* 204: 1016–1022.

Cheillan, D. (2020). Zellweger syndrome disorders: from severe neonatal disease to atypical adult presentation. *Adv. Exp. Med. Biol.* 1299: 71–80.

Ciniawsky, S., Grimm, I., Saffian, D., Girzalsky, W., Erdmann, R., and Wendler, P. (2015). Molecular snapshots of the Pex1/6 AAA+ complex in action. *Nat. Commun.* 6: 7331.

Denkert, N., Schendzielorz, A.B., Barbot, M., Versemann, L., Richter, F., Rehling, P., and Meinecke, M. (2017). Cation selectivity of the presequence translocase channel Tim23 is crucial for efficient protein import. *eLife* 6: 439.

Dodt, G., Braverman, N., Wong, C., Moser, A., Moser, H.W., Watkins, P., Valle, D., and Gould, S.J. (1995). Mutations in the PTS1 receptor gene, PXR1, define complementation group 2 of the peroxisome biogenesis disorders. *Nat. Genet.* 9: 115–125.

Domanska, G., Motz, C., Meinecke, M., Harsman, A., Papatheodorou, P., Reljic, B., Dian-Lothrop, E.A., Galmiche, A., Kepp, O., Becker, L., et al. (2010). Helicobacter pylori VacA toxin/subunit p34: targeting of an anion channel to the inner mitochondrial membrane. *PLoS Pathog.* 6: e1000878.

Emmanouilidis, L., Gopalswamy, M., Passon, D.M., Wilmanns, M., and Sattler, M. (2016). Structural biology of the import pathways of peroxisomal matrix proteins. *Biochim. Biophys. Acta* 1863: 804–813.

Erdmann, R. and Schliebs, W. (2005). Peroxisomal matrix protein import: the transient pore model. *Nat. Rev. Mol. Cell Biol.* 6: 738–742.

Gardner, B.M., Chowdhury, S., Lander, G.C., and Martin, A. (2015). The Pex1/Pex6 complex is a heterohexameric AAA+ motor with alternating and highly coordinated subunits. *J. Mol. Biol.* 427: 1375–1388.

Goldman, B.M. and Blobel, G. (1978). Biogenesis of peroxisomes: intracellular site of synthesis of catalase and uricase. *Proc. Natl. Acad. Sci. U.S.A.* 75: 5066–5070.

Gould, S.J., Keller, G.A., Hosken, N., Wilkinson, J., and Subramani, S. (1989). A conserved tripeptide sorts proteins to peroxisomes. *J. Cell Biol.* 108: 1657–1664.

Grou, C.P., Carvalho, A.F., Pinto, M.P., Wiese, S., Piechura, H., Meyer, H.E., Warscheid, B., Sá-Miranda, C., and Azevedo, J.E. (2008). Members of the E2D (UbcH5) family mediate the ubiquitination of the conserved cysteine of Pex5p, the peroxisomal import receptor. *J. Biol. Chem.* 283: 14190–14197.

Guan, L., Denkert, N., Eisa, A., Lehmann, M., Sjuts, I., Weiberg, A., Soll, J., Meinecke, M., and Schwenkert, S. (2019). JASSY, a chloroplast outer membrane protein required for jasmonate biosynthesis. *Proc. Natl. Acad. Sci. U.S.A.* 116: 10568–10575.

Hotz, T., Schütte, O.M., Sieling, H., Polupanow, T., Diederichsen, U., Steinem, C., and Munk, A. (2013). Idealizing ion channel recordings by a jump segmentation multiresolution filter. *IEEE Trans. Nanobioscience* 12: 376–386.

Kerssen, D., Hambruch, E., Klaas, W., Platta, H.W., de Kruijff, B., Erdmann, R., Kunau, W.H., and Schliebs, W. (2006). Membrane association of the cycling peroxisome import receptor Pex5p. *J. Biol. Chem.* 281: 27003–27015.

Kunze, M. (2020). The type-2 peroxisomal targeting signal. *Biochim. Biophys. Acta Mol. Cell Res.* 1867: 118609.

Kunze, M., Malkani, N., Maurer-Stroh, S., Wiesinger, C., Schmid, J.A., and Berger, J. (2015). Mechanistic insights into PTS2-mediated peroxisomal protein import: the co-receptor PEX5L drastically increases the interaction strength between the cargo protein and the receptor PEX7. *J. Biol. Chem.* 290: 4928–4940.

Lazarow, P.B. and Fujiki, Y. (1985). Biogenesis of peroxisomes. *Annu. Rev. Cell Biol.* 1: 489–530.

Meinecke, M., Bartsch, P., and Wagner, R. (2016). Peroxisomal protein import pores. *Biochim. Biophys. Acta Mol. Cell Res.* 1863: 821–827.

Meinecke, M., Cizmowski, C., Schliebs, W., Kruger, V., Beck, S., Wagner, R., and Erdmann, R. (2010). The peroxisomal importomer constitutes a large and highly dynamic pore. *Nat. Cell Biol.* 12: 273–277.

Montilla-Martinez, M., Beck, S., Klümper, J., Meinecke, M., Schliebs, W., Wagner, R., and Erdmann, R. (2015). Distinct pores for peroxisomal import of PTS1 and PTS2 proteins. *Cell Rep.* 13: 2126–2134.

Neuberger, G., Maurer-Stroh, S., Eisenhaber, B., Hartig, A., and Eisenhaber, F. (2003). Motif refinement of the peroxisomal targeting signal 1 and evaluation of taxon-specific differences. *J. Mol. Biol.* 328: 567–579.

Neuhaus, A., Kooshapur, H., Wolf, J., Meyer, N.H., Madl, T., Saidowsky, J., Hambruch, E., Lazam, A., Jung, M., Sattler, M., et al. (2014). A novel Pex14 protein-interacting site of human Pex5 is critical for matrix protein import into peroxisomes. *J. Biol. Chem.* 289: 437–448.

Otera, H., Harano, T., Honsho, M., Ghaedi, K., Mukai, S., Tanaka, A., Kawai, A., Shimizu, N., and Fujiki, Y. (2000). The mammalian peroxin Pex5pL, the longer isoform of the mobile peroxisome targeting signal (PTS) type 1 transporter, translocates the Pex7p/PTS2 protein complex into peroxisomes via its initial docking site, Pex14p. *J. Biol. Chem.* 275: 21703–21714.

Otera, H., Setoguchi, K., Hamasaki, M., Kumashiro, T., Shimizu, N., and Fujiki, Y. (2002). Peroxisomal targeting signal receptor Pex5p interacts with cargoes and import machinery components in a spatiotemporally differentiated manner: conserved Pex5p WXXXF/Y motifs are critical for matrix protein import. *Mol. Cell Biol.* 22: 1639–1655.

Platta, H.W., El Magraoui, F., Schlee, D., Grunau, S., Girzalsky, W., and Erdmann, R. (2007). Ubiquitination of the peroxisomal import receptor Pex5p is required for its recycling. *J. Cell Biol.* 177: 197–204.

Platta, H.W., Grunau, S., Rosenkranz, K., Girzalsky, W., and Erdmann, R. (2005). Functional role of the AAA peroxins in dislocation of the cycling PTS1 receptor back to the cytosol. *Nat. Cell Biol.* 7: 817–822.

Rucktäschel, R., Girzalsky, W., and Erdmann, R. (2011). Protein import machineries of peroxisomes. *Biochim Biophys Acta.* 1808: 892–900.

Saffert, P., Enenkel, C., and Wendler, P. (2017). Structure and function of p97 and Pex1/6 type II AAA+ complexes. *Front. Mol. Biosci.* 4: 33.

Saidowsky, J., Dodt, G., Kirchberg, K., Wegner, A., Nastainczyk, W., Kunau, W.H., and Schliebs, W. (2001). The di-aromatic pentapeptide repeats of the human peroxisome import receptor PEX5 are separate high affinity binding sites for the peroxisomal membrane protein PEX14. *J. Biol. Chem.* 276: 34524–34529.

Schliebs, W. and Kunau, W.H. (2006). PTS2 co-receptors: diverse proteins with common features. *Biochim. Biophys. Acta* 1763: 1605–1612.

Smart, O.S., Breed, J., Smith, G.R., and Sansom, M.S. (1997). A novel method for structure-based prediction of ion channel conductance properties. *Biophys. J.* 72: 1109–1126.

Swinkels, B.W., Gould, S.J., Bodnar, A.G., Rachubinski, R.A., and Subramani, S. (1991). A novel, cleavable peroxisomal targeting signal at the amino-terminus of the rat 3-ketoacyl-CoA thiolase. *EMBO J.* 10: 3255–3262.

Tarasenko, D., Barbot, M., Jans, D.C., Kroppen, B., Sadowski, B., Heim, G., Möbius, W., Jakobs, S., and Meinecke, M. (2017). The MICOS component Mic60 displays a conserved membrane-bending activity that is necessary for normal cristae morphology. *J. Cell Biol.* 216: 889–899.

van den Bosch, H., Schutgens, R.B., Wanders, R.J., and Tager, J.M. (1992). Biochemistry of peroxisomes. *Annu. Rev. Biochem.* 61: 157–197.

Vasic, V., Denkert, N., Schmidt, C.C., Riedel, D., Stein, A., and Meinecke, M. (2020). Hrd1 forms the retrotranslocation pore regulated by auto-ubiquitination and binding of misfolded proteins. *Nat. Cell Biol.* 22: 274–281.

Walton, P.A., Hill, P.E., and Subramani, S. (1995). Import of stably folded proteins into peroxisomes. *Mol. Biol. Cell* 6: 675–683.

Wanders, R.J.A. (2018). Peroxisomal disorders: Improved laboratory diagnosis, new defects and the complicated route to treatment. *Mol. Cell. Probes* 40: 60–69.

Wanders, R.J.A., Waterham, H.R., and Ferdinandusse, S. (2018). Peroxisomes and their central role in metabolic interaction networks in humans. *Subcell. Biochem.* 89: 345–365.

Waterham, H.R., Ferdinandusse, S., and Wanders, R.J. (2016). Human disorders of peroxisome metabolism and biogenesis. *Biochim. Biophys. Acta* 1863: 922–933.

---

**Supplementary Material:** The online version of this article offers supplementary material (<https://doi.org/10.1515/hsz-2022-0170>).